Hypercoordinate Diorganosilanes Featuring an ⟨*ONO*⟩ Tridentate Ligand. A Surprising Equilibrium Between Penta- and Tetracoordination

Jörg Wagler[a] and Erica Brendler[b]

[a] Institut für Anorganische Chemie, Technische Universität Bergakademie Freiberg, Leipziger Str. 29, D-09596 Freiberg, Germany
[b] Institut für Analytische Chemie, Technische Universität Bergakademie Freiberg, Leipziger Str. 29, D-09596 Freiberg, Germany

Reprint requests to Dr. Jörg Wagler. Fax: (+49) 3731 39 4058.
E-mail: joerg.wagler@chemie.tu-freiberg.de

Z. Naturforsch. **2007**, *62b,* 225 – 234; received June 23, 2006

The reaction of the tridentate ligand-precursor molecule **1**, *o*-HO-*p*-MeO-C_6H_3-C(Ph)=N-(*o*-C_6H_4)-OH, with diorganodichlorosilanes Me_2SiCl_2, Ph_2SiCl_2 and $PhAllSiCl_2$ yields pentacoordinate silicon complexes R,R′Si[*o*-O-*p*-MeO-C_6H_3-C(Ph)=N-(*o*-C_6H_4)-O] (**2a′**: R, R′ = Me; **2b**: R, R′ = Ph; **2c**: R = Ph, R′ = All). **2b** and **2c** have pentacoordinate silicon atoms in the solid state as well as in chloroform solution. Surprisingly, for **2a** an isomer **2a′** with Si-tetracoordination is preferred in the solid state, while the Si-pentacoordinated isomer **2a** may dominate in solution. The hypercoordinate allylsilane **2c** with a C=X → Si moiety is stable in solution and does not undergo a 1,3-allyl-shift-reaction.

Key words: Allyl, Chelate, Equilibrium, Hypercoordination, Silicon

Introduction

The chemistry of complexes with hypercoordinate silicon atoms is interesting from many points of view. Silanes with electron-withdrawing substituents (*e. g.* Cl, F, CF_3) in particular are likely to form hypercoordinate complexes [1]. With chelating ligands coordination numbers higher than 4 at the silicon atom are favoured even if it is bearing only less electron-withdrawing substituents. Although pentacoordinate Si complexes with up to five carbon donor atoms have already been synthesized by Kolomeitsev *et al.* [2] and Lammertsma *et al.* [3], there is still a high interest in the enhanced chemical reactivity and its relationship to the structure of the hypercoordinate organosilanes. Due to the increased coordination number of the Si atom, the Si-C bonds may be significantly activated and the complexes may be useful reagents in organic synthesis. Palladium-catalyzed cross-coupling reactions with difluorotriphenylsilicate [4], allyl shift reactions with hypercoordinate allylsilanes as intermediates [5] and photochemically induced 1,3-organyl-shift reactions [6] were reported (Scheme 1).

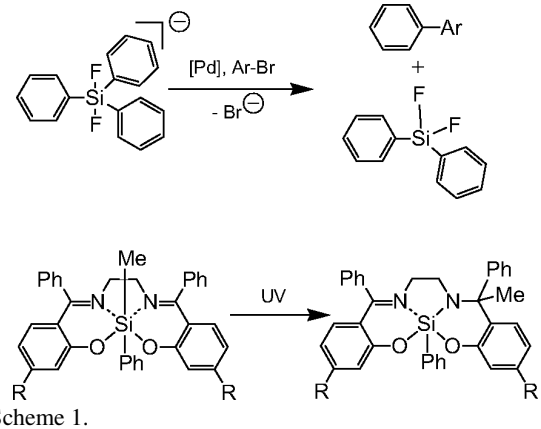

Scheme 1.

The control of the Si atom's coordination behavior by subtle differences in electronic effects of the Si-bonded organyl groups is also a challenging field of research [7]. Recently, we reported the syntheses of various hexacoordinate diorganosilanes with tetradentate ⟨*ONNO*⟩-chelating salen-type ligands and Si-C bond cleavage reactions [6, 8, 9]. The switch to an ⟨*ONO*⟩-chelating tridentate ligand system led to new insights into both the C=N → Si coordination and the activation of the Si-C bond by hypercoordination.

Results and Discussion

The tridentate ligand-precursor molecule **1** (Scheme 2, top) was prepared from 2-hydroxy-4-methoxy-

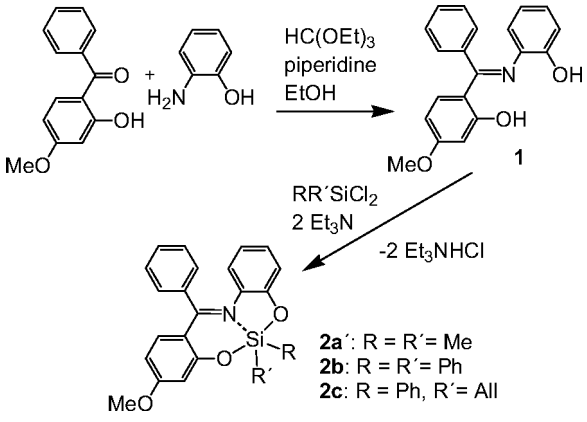

Scheme 2.

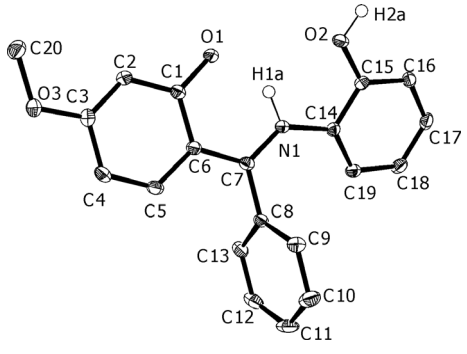

Fig. 1. Molecular structure of **1** (ORTEP plot with 50 % probability ellipsoids, carbon-bound hydrogen atoms omitted).

benzophenone and *o*-aminophenol. Its crystal structure is presented in Fig. 1.

The acidic hydrogen atoms H1a and H2a were found on residual electron density maps. H1a is situated in a hydrogen bridge position between O1 and N1 in closer proximity of the nitrogen atom. Since the donor site of N1 is thus occupied, the O2-H2a bond is directed away from it. In comparison with the bond C15-O2 [1.357(1) Å], the bond C1-O1 [1.294(1) Å] is quite short. The location of H1a close to N1, the short bond C1-O1 as well as the alternating bond lenghts from C1 to C7 (depicted in Scheme 3, left) suggest a significant contribution of the *o*-quinoid structure drawn in Scheme 3.

Compound **1** was reacted with Me_2SiCl_2, Ph_2SiCl_2 and $PhAllSiCl_2$ in the presence of triethylamine as a supporting base to yield **2a** / **2a′**, **2b** and **2c**, respectively (Scheme 2, bottom).

The reaction with dimethyldichlorosilane in thf yields complex **2a**, which exhibits a tetracoordinate silicon atom, as well as its isomer **2a′**, in which the silicon atom is pentacoordinated (Scheme 4). Complex **2a** was isolated as an almost colorless crystalline solid which proved to be the pure isomer with a tetracoordinate Si-atom (^{29}Si CP/MAS NMR: $\delta = -6.3$ ppm, single crystal X-ray diffraction: see Fig. 2). However, this tetracoordination is not maintained in chloroform solution, where an equilibrium between the two coordination modes is established (Scheme 4).

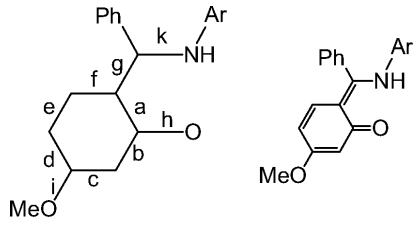

Scheme 3. Bond lengths in Å: a) 1.445(2), b) 1.422(2), c) 1.373(2), d) 1.417(2), e) 1.367(2), f) 1.424(2), g) 1.433(2), h) 1.294(1), i) 1.362(1), k) 1.323(1).

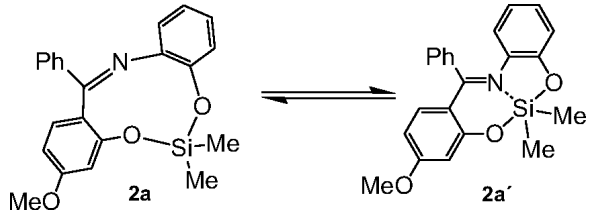

Scheme 4.

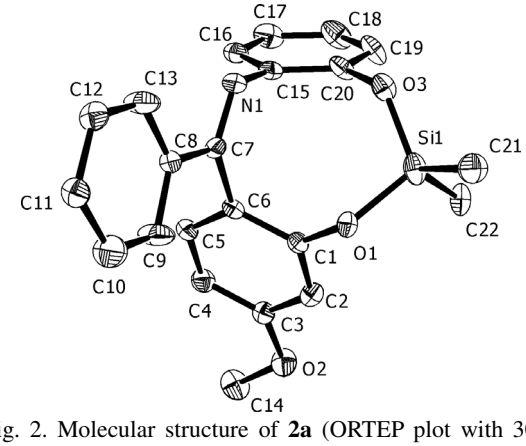

Fig. 2. Molecular structure of **2a** (ORTEP plot with 30 % probability ellipsoids, hydrogen atoms omitted).

In the crystal the molecules **2a** are disordered in 1 : 1 ratio (see X-ray structure analyses section). Although the quality of the structure **2a** is notably lower than those of **2b** and **2c**, many parts of the disordered molecules are well separated and some interesting structural features can be discussed. Due to

Table 1. Data of crystal structure determination and refinement of **1**, **2a**, **2b** and **2c**.

Compound	**1**	**2a**	**2b**	**2c**
Empirical formula	$C_{20}H_{17}NO_3$	$C_{22}H_{21}NO_3Si$	$C_{32}H_{25}NO_3Si$	$C_{29}H_{25}NO_3Si$
T (K)	93(2)	93(2)	90(2)	296(2)
Crystal system	monoclinic	triclinic	monoclinic	triclinic
Space group	$P2_1/c$	$P\bar{1}$	$P2_1/n$	$P\bar{1}$
a (Å)	13.2801(8)	6.7311(6)	11.0142(3)	8.6034(3)
b (Å)	8.5246(5)	11.6420(11)	14.4717(4)	10.0242(3)
c (Å)	14.1406(8)	12.6761(12)	15.6984(5)	14.8781(5)
α (°)	90	90.062(5)	90	99.509(1)
β (°)	101.312(1)	90.029(5)	101.217(1)	106.328(1)
γ (°)	90	98.585(5)	90	93.228(1)
Z, V (Å^3)	4, 1569.72(16)	2, 982.21(16)	4, 2454.43(12)	2, 1207.27(7)
ρ_{calc} (g cm^{-3}), μ (mm^{-1})	1.351, 0.091	1.270, 0.141	1.352, 0.132	1.275, 0.129
$F(000)$	672	396	1048	488
Crystal size (mm^3)	$0.40 \times 0.22 \times 0.05$	$0.30 \times 0.20 \times 0.15$	$0.60 \times 0.45 \times 0.20$	$0.58 \times 0.30 \times 0.18$
$2\theta_{max}$ (°)	56	51	80	55
Index ranges	$-17 \le h \le 17$, $-11 \le k \le 11$, $-18 \le l \le 18$	$-8 \le h \le 8$, $-14 \le k \le 13$, $-15 \le l \le 12$	$-17 \le h \le 19$, $-26 \le k \le 25$, $-28 \le l \le 28$	$-11 \le h \le 11$, $-12 \le k \le 8$, $-19 \le l \le 19$
Reflections collected, R_{int}	17573, 0.0298	8488, 0.0257	92085, 0.0255	14338, 0.0192
Independent reflections	3762	3609	15181	5500
Parameters	223	439	335	314
R Indices [$I \ge 2\sigma(I)$]	$R_1 = 0.0369$, $wR_2 = 0.0942$	$R_1 = 0.0633$, $wR_2 = 0.1316$	$R_1 = 0.0361$, $wR_2 = 0.1098$	$R_1 = 0.0402$, $wR_2 = 0.1130$
R Indices (all data)	$R_1 = 0.0481$, $wR_2 = 0.0993$	$R_1 = 0.1040$, $wR_2 = 0.1430$	$R_1 = 0.0445$, $wR_2 = 0.1154$	$R_1 = 0.0560$, $wR_2 = 0.1208$
Largest diff. peak and hole (e Å^{-3})	0.328, −0.186	0.286, −0.261	1.033, −0.550	0.269, −199

the tetracoordination of the Si atom, the Si-O bonds (Si1-O1 1.651(5) Å, Si1-O3 1.658(6) Å) are significantly shorter than in **2b** and **2c** (compare Table 1). The C=N bond (C7=N1 1.285(7) Å) is slightly shorter than in **2b** and **2c**. This is to be expected as in the absence of Si-N coordination the C=N bond is strengthened. The lone pair of N1 appears to point out of the molecule. Thus, the interaction of this lone pair with hydrogen bridge donors (*e. g.* a chloroform molecule) may support the Si-N dissociation with formation of the tetracoordinate isomer **2a**. The tetracoordination of the Si atom in **2a** in the solid state may also be due to the lower solubility of this isomer. In order to prove the hypothesis that chloroform supports the configuration with a tetracoordinate Si atom as it has been found in another case of (imine)N → Si coordination equilibrium [10], the ^{29}Si NMR spectrum of **2a** was also recorded in toluene-d$_8$ and dmso-d$_6$ at ambient temperature. The concentration ratio tetra- : pentacoordinate isomer was found to be solvent dependent: 1.7 in $CDCl_3$, 0.9 in toluene-d$_8$, 3.0 in dmso-d$_6$. The high content of the tetracoordinate isomer in dmso-solution indicates the domination of this isomer in polar solvents even if they are not hydrogen bond donors. Surprisingly, in each case the isomer with the tetracoordinate silicon atom produces two ^{13}C as well as ^{1}H NMR signals for the Si-bonded methyl groups while there is only one Si-CH$_3$ signal for the species with the pentacoordinate Si atom. (In $CDCl_3$ coincidence of the two diastereotopic ^{1}H (Si-CH$_3$) NMR signals is achieved at r. t., see experimental section.) In both the isomers with tetra- and some isomers with pentacoordinate Si atoms the Si-bonded methyl groups are diastereotopic. In case of TBP coordination with an O-Si-O axis and equatorially situated Si-C bonds, the Si-CH$_3$ groups are chemically equivalent. Such coordination has been observed in a silicon complex of ligand **1** bearing Si-N, Si-CH$_3$ and Si-Si bonds in equatorial positions [11] and may therefore be taken into account as one reason for the emerging of only one ^{1}H and ^{13}C NMR Si-CH$_3$ signal for the component **2a**′. The presence of other arrangements of the five donor atoms together with rapid configurational exchange, however, can also be taken into account. The configurational exchange of each of the isomers with the tetracoordinate silicon atom seems to be slow on the NMR time scale.

For a closer insight into the equilibrium between the isomers **2a** and **2a**′, ^{1}H and ^{29}Si(INEPT) NMR spectra of a solution of **2a** in toluene-d$_8$ were recorded at vari-

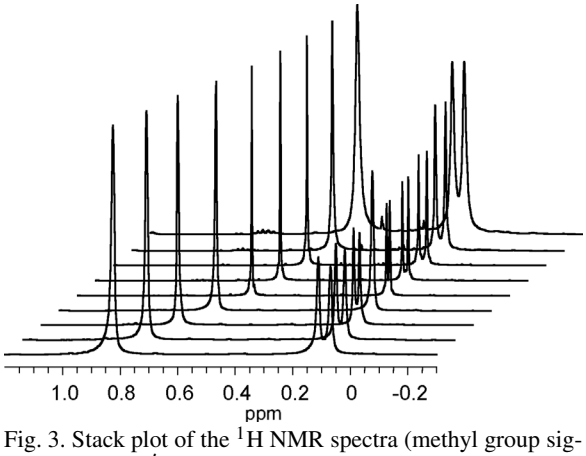

Fig. 3. Stack plot of the ^{1}H NMR spectra (methyl group signals) of **2a** / **2a′** in toluene-d$_8$ at various temperatures (from front to back [°C]: −30, −20, −10, 5, 20, 30, 40, 50, 60).

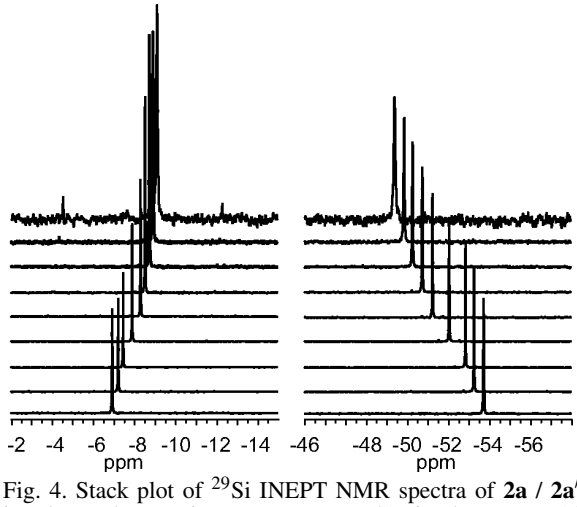

Fig. 4. Stack plot of ^{29}Si INEPT NMR spectra of **2a** / **2a′** in toluene-d$_8$ at various temperatures. Section between −14 and −46 ppm omitted for clarity, from front to back [°C]: −30, −20, −10, 5, 20, 30, 40, 50, 60.

ous temperatures (Figs. 3 and 4). The ^{1}H NMR signals of the Si-bonded methyl groups of the tetra- and pentacoordinate isomers are well separated in the spectrum and can be used to determine the concentration ratio of the isomers. One of the two singlets of the tetracoordinate isomer changes its ^{1}H NMR shift in such a way that coincidence of the singlets is reached at 5 °C. At higher temperatures, however, these signals separate again, indicating that coalescence has not been achieved.

Assuming an equilibrium as given in Scheme 4, $\ln K$ *vs.* $1/T$ were plotted and ΔH and ΔS for the dissociation were estimated from the equation $\ln K = -(\Delta H/\mathrm{R} \cdot 1/T) + (\Delta S/\mathrm{R})$ and the linearization of the

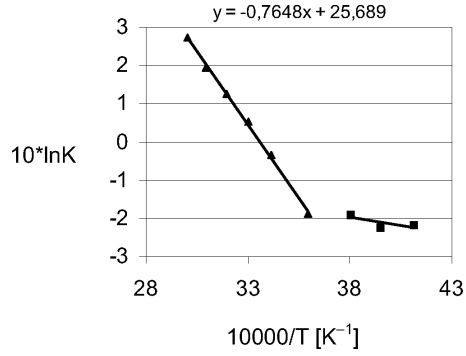

Fig. 5. Linearized plot of ln(K) *vs.* $1/T$ for the equilibrium between **2a′** with penta- and its isomer **2a** with tetracoordinate Si atom.

$\ln K$ *vs.* $1/T$ plot ($y = -764.8x + 2.569$, Fig. 5). A striking kink in the $\ln K$ *vs.* $1/T$ plot at about 5 °C suggests that below this temperature level the equilibration process is disturbed by a kinetic barrier. (Thus, only the data from 5 °C to 60 °C were taken into account for thermodynamic analysis of the equilibration processes between the isomers with tetra- and pentacoordinate Si-atom.)

The thermodynamic data obtained (**2a′** → **2a** dissociation: ΔH = 6.36 kJ/mol, ΔS = 21.4 J/molK) indicate a small enthalpy gain (−6.36 kJ/mol) by N → Si bond formation. This value is much smaller than the −31.5 kJ/mol which were found for complexation of the Si atom with a bidentate 2-iminomethylphenolate ligand and an $\langle OO'NC(sp^2)\rangle$-donor situation at the Si-atom [10]. The N → Si bond dissociation in **2a** seems to be facilitated by the special bonding pattern of ligand **1**. The phenyl group of the 2-oxybenzophenoneimine provides a π-electron system, which may interact with the imine double bond's π-electron system only in the tetracoordinate silicon complex (see Fig. 2, top, C7=N1 in conjugation with phenyl C8 - C13) but not in a pentacoordinate Si-complex (compare with Figs. 6 and 7). Finally, the lower Lewis acidity of the Si centre with its two electron rich methyl substituents weakens any additional N → Si donor action. The entropy change (21.4 J/molK for the Si-N dissociation reaction) appears to be associated with the relatively rigid chelate systems in both isomers.

Beside the kink in the $\ln K$ *vs.* $1/T$ plot at 5 °C, two other notable features of this equilibrium are the coincidence of the Si-CH$_3$ ^{1}H NMR signals of the tetracoordinate isomer at 5 °C as well as the different shift rates $\Delta\delta^{29}$Si of the signals which represent

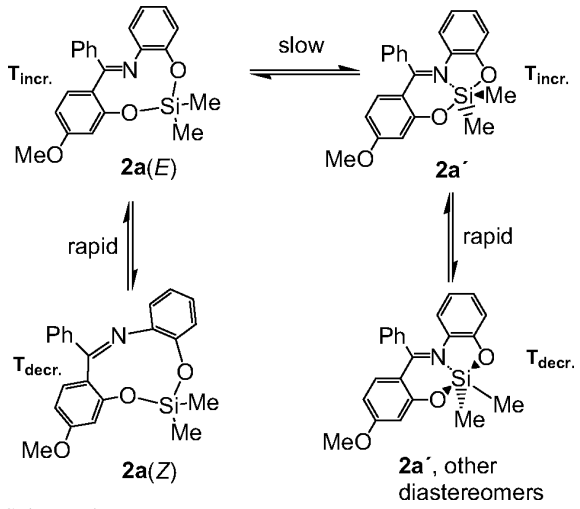

Scheme 5.

tetracoordinate ($\Delta\delta^{29}$Si = −0.030 to −0.018 ppmK^{-1}) and pentacoordinate silicon complexes ($\Delta\delta^{29}$Si = 0.048 ppmK^{-1}, steady shift). The latter two features indicate the superposition of more than one configurational exchange processes. Both ^{29}Si NMR signals exhibit temperature dependent shifts. For slow exchange processes between two species only a change in intensities is to be expected [7b, c]. An explanation of the observations can be that both coordination modes include more than one isomer which undergo rapid interconversion and lead to one representative signal for each coordination number. The chemical shift of each of these signals is then defined by the ratio of the contributions from the rapidly interconverting diastereomers [10, 12]. A comparison between the molecular structures of **2a** and **2b**, **2c** (Figs. 6 and 7) reveals that the C=N moiety of the tridentate ligand system has *Z* configuration in **2a** and *E* configuration in the pentacoordinate Si-complexes **2b** and **2c**. Therefore, one can discuss an isomer **2a**(*E*) (featuring a tetracoordinate Si-atom and *E* configuration of the imine system) as an intermediate between the tetracoordinate silicon complex **2a**(*Z*) and the pentacoordinate species **2a**′. The temperature dependent ^{1}H and ^{29}Si NMR properties of the solution of **2a**/**2a**′ can be explained assuming the equilibria which are depicted in Scheme 5 as a simple model (superposition of additional exchange processes can not be excluded).

Interconversions between the potential isomers with tetracoordinate Si-atom (*E*/*Z*-isomerization at the C=N moiety) must be rapid on the NMR time scale, thus leading to only one representative ^{29}Si NMR signal for all species featuring this coordination number. The rapid exchange processes of pentacoordinate silicon complexes have already been mentioned. The exchange between tetra- and pentacoordination, however, is slow and gives rise to two distinct signals, one for each coordination number.

The rapid exchange between **2a**(*E*) and **2a**(*Z*) (with **2a**(*E*) favored at the higher temperature level) can account for the shift of their ^{29}Si NMR signals to higher field at higher temperatures: In **2a**(*E*) the tetrahedral coordination sphere of the Si-atom may be N-capped with the ^{29}Si nucleus better shielded.

The isomers with tetracoordinate Si-atom represent macrocycles (9-membered ring systems). Both of them bear diastereotopic Si-CH$_3$ groups, which may equilibrate by ring inversion processes to achieve chemical equivalence on the NMR time scale. These exchange processes seem to be NMR-slow, thus leading to two ^{1}H and ^{13}C NMR resonances, respectively, for the isomers with tetracoordinate Si-atom. Temperature dependent changes in the molar fractions of rapidly exchanging isomers **2a**(*E*) and **2a**(*Z*) could cause shifts of the weighted avarage ^{1}H resonances. The assumption that the ^{1}H resonance of one of the diastereotopic Si-CH$_3$ groups is much more influenced by the *E*/*Z* isomerization than that of the other Si-CH$_3$ group provides an explanation for the striking change of one of the ^{1}H NMR signals beyond coincidence.

Taking into account that all isomerization processes among the isomers with tetracooordinate Si-atom are rapid on the NMR time scale (1 ^{29}Si signal only!), *slow* ring inversion, which leads to identical species with diastereotopic Si-CH$_3$ groups, is the only process which can cause the emerging of two ^{1}H and ^{13}C NMR signals for the Si-CH$_3$ groups of these tetracoordinate silicon compounds. According to the slow and rapid isomerization processes in our model (Scheme 5), this ring inversion may occur *via* the pentacoordinate silicon complex **2a**′, meaning that the rapid transitions from **2a**(*Z*) to **2a**(*E*) and back must be accompanied by the return of the diastereotopic Si-CH$_3$ groups into their initial positions exclusively.

The ^{29}Si NMR signal of the pentacoordinate species also depends on the temperature (Fig. 4). Increasing temperature causes a shift of the ^{29}Si NMR signals towards each other (as well as a discernible broadening of the signals at 60 °C, however far away from coalescence). This observation as well as the shift of the ^{1}H NMR signal of the Si-CH$_3$ protons in the pentaco-

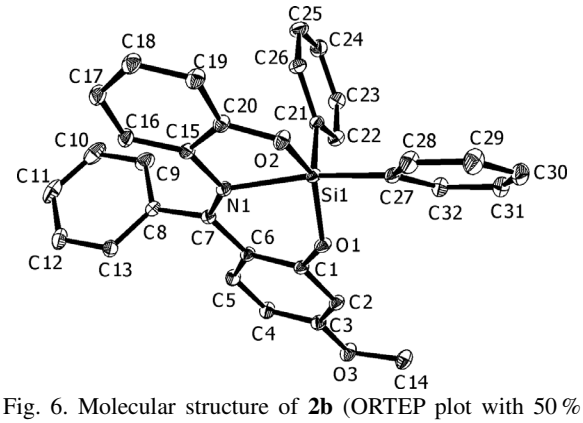

Fig. 6. Molecular structure of **2b** (ORTEP plot with 50 % probability ellipsoids, hydrogen atoms omitted).

ordinate isomer(s) to lower field at lower temperatures can be explained with a rapid interconversion of two or more pentacoordinate diastereomers (as depicted in Scheme 5) or increasing N → Si coordination strength at lower temperature levels. Both, the favored formation of TBP shaped silicon complexes bearing an axially situated Si-CH_3 group as well as the shortening of the N → Si bond distance, which are accompanied with a lengthening of the average Si-C bond distance, could result in a better shielding of the ^{29}Si nucleus as well as decreased shielding of the Si-CH_3 protons at lower temperatures. Thus, one can not exclude one of these possibilities.

Different coordination behavior was found with **2b** and **2c**. **2b**, recrystallized from thf, forms light yellowish-orange colored crystals suitable for X-ray analysis (Fig. 6).

The silicon atom is situated in a coordination geometry which is almost midway between trigonal bipyramid (TBP) and square pyramid (SQP): 47 % TBP with N1 and C27 in axial positions and the oxygen atoms O1 and O2 in equatorial positions. C21 can be referred to either as part of the equator of a TBP or as the top of the SQP. The Si-N bond 2.107(1) Å is quite long in comparison with Si-N(sp^2) bonds in hexacoordinate diorganosilanes with salen-like ligands (*ca.* 1.98 – 2.00 Å, see [8]). The decrease in coordination number should be accompanied by a decrease in bond lengths to the same sort of atoms. The reason for the contrasting behavior in case of **2b** can be found if the relative position of the Si-N bond is taken into account. While in hexacoordinate diorganosilanes with salen-type ligands the Si-N bonds are *trans* to Si-O bonds, the Si-N bond in **2b** is *trans* (N1-Si1-C27 165.6(1)°) to a Si-C bond. The lower

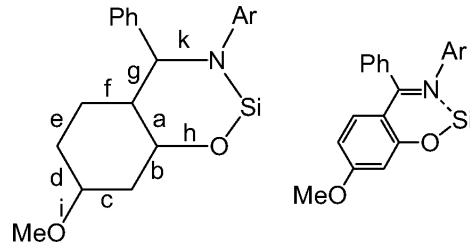

Scheme 6. Bond lengths in Å: a) 1.408(1), b) 1.401(1), c) 1.394(1), d) 1.406(1), e) 1.374(1), f) 1.413(1), g) 1.447(1), h) 1.349(1), i) 1.353(1), k) 1.307(1).

electronegativity of the carbon atom gives rise to a less Lewis-acidic σ*-MO which is expected to be essential for the interaction with the *trans*-situated donor atom. The Si-C bonds in **2b** (Si1-C21 1.878(1) Å, Si1-C27 1.906(1) Å), however, are significantly shorter than those of the hexacoordinate diorganosilanes mentioned above (*ca.* 1.93 – 1.97 Å). A slight but significant difference in the distances Si1-C21 and Si1-C27 is based on their different location in the Si coordination sphere.

Surprisingly, the Si-O bonds (Si1-O1 and Si1-O2 1.700(1) Å) have the same length, although O1 is part of a six- and O2 is part of a five-membered chelate.

Referring to the interesting bonding situation in the free ligand acid **1** (see Scheme 3), the analogous C-C bonds are less alternating in the silicon complex **2b** (Scheme 6, left) and the bonds C1-O1 (1.349(1) Å) as well as C7-N1 (1.307(1) Å) are also lengthened and shortened, respectively. This result allows the conclusion that the oxophilic silicon atom reduces the *o*-quinoid character of the ligand illustrated in Scheme 3. In chloroform solution the pentacoordination of the Si atom of **2b** is retained (δ^{29}Si = −84.6 ppm).

A solution of **2b** in THF was irradiated with UV light for 6 h (reaction conditions see ref. [6]) but no indication for Si-C bond cleavage and 1,3-shift of a phenyl group was found. The Si-C bond Si1-C27 (1.906(1) Å) is significantly longer than the Si-C bonds in some previously published pentacoordinate Si complexes with salen-like ligands. This slight plus in Si-C bond activation appears to be not enough to allow any UV-stimulated organylation of the imine carbon atom.

Compound **2c** was prepared in a similar manner. Suitable crystals for X-ray analysis were obtained from diethylether/pentane (Fig. 7).

Table 2. Selected bond lengths [Å] and angles [°] of **2b** and **2c**.

	2b	**2c**
Si1-O1	1.700(1)	1.711(1)
Si1-O2	1.700(1)	1.713(1)
Si1-N1	2.107(1)	2.058(1)
Si1-C21	1.878(1)	1.875(2)
Si1-C27	1.906(1)	1.907(2)
C7-N1	1.307(1)	1.312(2)
C1-O1	1.349(1)	1.341(2)
N1-Si1-C27	165.6(1)	160.1(1)
O1-Si1-O2	137.2(1)	142.7(1)
O1-Si1-C21	111.2(1)	107.3(1)
O2-Si1-C21	108.9(1)	108.3(1)

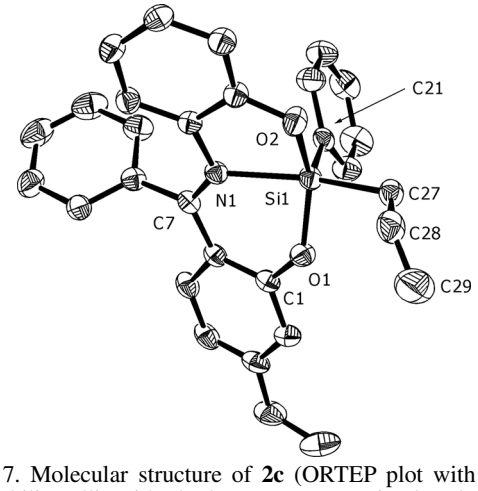

Fig. 7. Molecular structure of **2c** (ORTEP plot with 30 % probability ellipsoids, hydrogen atoms omitted). The allyl group is disordered over two sites (ratio 9 : 1). Only the dominating part is depicted.

Analogous to the situation in **2b**, the Si atom of **2c** is also situated in a coordination geometry on the way from TBP to SQP, but closer to a square pyramidal arrangement of the donor atoms (O1, O2, N1 and C27 in the base and C21 on top of the pyramid; 29 % TBP, compare Table 2). This transition towards an SQP coordination geometry is mainly caused by changes in the angles O1-Si1-O2, O1-Si1-C21 and N1-Si1-C27 (see Table 2). Surprisingly, the sp^3-hybridized carbon atom C27 is located opposite to the imine N atom N1, which causes a slightly longer Si-C-bond Si1-C27 (1.907(2) Å) than to the sp^2-hybridized phenyl carbon atom (Si1-C21: 1.875(2) Å). Generally a carbon atom of a phenyl moiety has a higher electronegativity than an sp^3-hybridized allyl carbon atom. Therefore, an interaction between the lone pair of imine nitrogen atom N1 and the σ^* orbital of the bond Si1-C21 should be preferred. The arrangement in

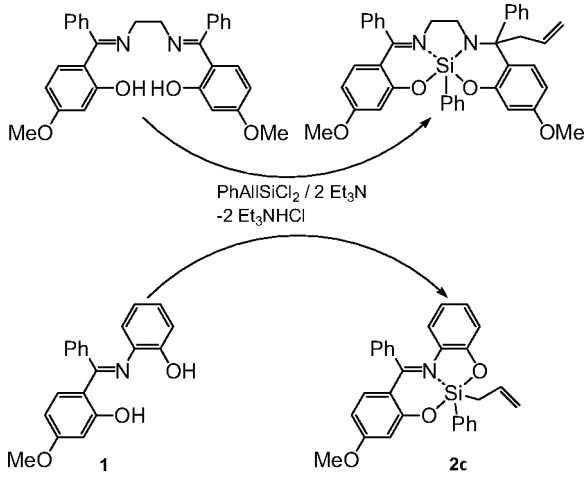

Scheme 7.

the crystal may be due to reasons of molecular packing. To the best of our knowledge, this is the only structurally confirmed example of a hypercoordinate Si-complex with N → Si donor action in *trans*-position to an sp^3-hybridized monodentate carbon substituent in the presence of a monodentate sp^2-hybridized carbon substituent so far. Due to the position of the donor atoms N1 and C27 in a SQP geometry, the bond length Si1-N1 (2.058(2) Å) is significantly shorter than the Si-N bond in **2b** (2.107(1) Å). The opposite Si-C bonds (Si1-C27 in both cases) are not influenced by this modified donor situation. The other features of the molecular structure of **2c** are similar to those of **2b** (*e. g.* similar bond lenghts Si1-O1 and Si1-O2 and throughout the tridentate ligand system as depicted in Scheme 6).

^{1}H, ^{13}C and ^{29}Si NMR spectra of **2c** were recorded. The intense peak at −76.2 ppm in the ^{29}Si NMR spectrum indicates the presence of the pentacoordinate silicon complex also in solution. In comparison with the spectrum of **2b**, the significant low field shift mainly originates from the substitution of an sp^2-hybridized for an sp^3-hybridized Si-bound carbon atom. This finding allows the conclusion that the Si-C bond in pentacoordinate allylsilanes with $\langle ONO \rangle$-chelating ligands is not activated enough for a rearrangement to an imine carbon atom as reported for tetradentate $\langle ONNO \rangle$-chelating ligands (Scheme 7) [9]. The ^{13}C NMR spectrum of **2c** consists of only 25 signals. As previously reported [6], the phenyl rotation in oxybenzophenoneimine ligands is slow on the NMR time scale. Therefore, diastereotopic *o*- and *m*-carbon atoms of this group are expected in **2c**. They should give rise to a sum of 27 ^{13}C NMR signals. The chemical identity of

these *o*- and *m*-carbon atoms is conditioned by either a rapid configurational inversion around the Si atom in **2c** or by coincidence of signals.

So far, only few examples of hypercoordinate silicon complexes with ⟨*ONO*⟩-chelating ligands of the 2-iminomethylenolate type were reported. Pentacoordinate Si complexes derived from the *N*-*o*-hydroxyphenylimine of acetylacetone, the structures of which were characterized by Tacke *et al.*, exhibit TBP configurations with the N atom of the tridentate ligand in axial position [13]. Another kind of ⟨*ONO*⟩-chelating ligands, pyridine-2,6-dimethanols and -diethanols, have also been reported to form pentacoordinate diorganosilanes with more or less intense N → Si donor action and trigonal bipyramidal coordination [14].

Conclusions

The complexation of various diorganodichlorosilanes with the tridentate ⟨*ONO*⟩-ligand **1** allows new insights into the reactivity of hypercoordinate silicon compounds. Pentacoordinate Si complexes exhibit increased reactivities due to both the higher coordination number of the Si atom as well as its vacancy for additional donor atoms [1]. Regarding intramolecular rearrangements such as 1,3-shifts of organyl groups, a line could be drawn between highly reactive hexacoordinate Si complexes with a tetradentate ⟨*ONNO*⟩-ligand system, and their inert counterparts with a tridentate ⟨*ONO*⟩-ligand and a pentacoordinate silicon atom. The characterization of Si complexes with ligand **1** illustrates the coordination behavior of this kind of chelating agents which leads to a coordination equilibrium between penta- and tetracoordinate Si-complexes in solution. An isomer with the lower Si coordination number is found in the solid state. Coordination motifs in the pentacoordinate silicon complexes are midway between TBP and SQP. A correlation between increasing TBP character of the Si coordination with increasing electronegativity of the "axially" situated monodentate substituent was found for complexes **2b** and **2c** as well as in structurally related compounds [11].

Experimental Section

Commercially available reagents were used. All manipulations were carried out under an inert atmosphere of dry argon. Triethylamine was distilled from calcium hydride and stored over molecular sieve 3 Å. Chloroform (stabilized with amylene) was dried over molecular sieve 3 Å. Ether, thf, hexane and pentane were distilled from sodium/benzophenone and stored over sodium wire. Solution NMR spectra were recorded on a BRUKER DPX 400 instrument ($CDCl_3$ solutions with TMS as internal standard), solid state spectra on a BRUKER Avance 400WB spectrometer using a 7 mm CP/MAS probehead (ν_{spin} = 5 kHz). Elemental analyses were carried out on a Foss Heraeus CHN-O-Rapid instrument.

1: Procedure following a literature method [15]: In dry ethanol (90 mL) 2-hydroxy-4-methoxybenzophenone (22.6 g, 99.3 mmol) and 2-aminophenol (10.8 g, 99.3 mmol) were dissolved under reflux and piperidine (8.76 g, 103 mmol) as well as triethylorthoformate (11.7 g, 79.1 mmol) were added. The resulting mixture was refluxed for 24 h, then the solvent was distilled off and the residue was recrystallized from isopropanol (100 mL) to yield an orange crystalline powder which was filtered off, washed with isopropanol and dried at 70 °C. Yield: 12.5 g (39.4 %, 39.1 mmol), m. p. 190 °C. – ^{1}H NMR (400 MHz, $CDCl_3$): δ = 3.82 (s, 3H, O-CH_3), 5.51 (s, 1H, ar OH), 6.30 – 7.40 (12H, ar), 14.26 (s, 1H, ar OH). – ^{13}C NMR (101 MHz, $CDCl_3$): δ = 55.5 (O-CH_3), 101.4, 106.7, 113.6, 115.3, 119.9, 122.6, 126.2, 128.3, 128.6, 129.4, 133.6, 133.9, 134.1 (ar), 149.0, 164.4, 165.9, 175.5 (ar C-O, C=N). – $C_{20}H_{17}NO_3$ (319.36): calcd. C 75.22, H 5.37, N 4.39; found C 75.21, H 5.12, N 4.45.

2a / (**2a′**): In thf (30 mL) ligand **1** (2.00 g, 6.25 mmol) and triethylamine (1.90 g, 18.8 mmol) were stirred at −10 °C and a solution of dimethyldichlorosilane (0.85 g, 6.59 mmol) in thf (20 mL) was added dropwise within 15 min. The resulting orange mixture was stirred at −10 °C for further 15 min, then the triethylamine hydrochloride was filtered off and washed with thf (20 mL). The volatiles were removed from the filtrate under reduced pressure. Then the oily residue was dissolved in chloroform (1.5 mL) and *n*-hexane (4 mL) was added. This solution was stored at 8 °C for 10 d, then the colorless crystalline product **2a** was filtered off and washed with hexane (5 mL) and dried in a vacuum. The filtrate was stored at −18 °C to yield a second crop of colorless crystals of **2a**. Yield: 1.05 g (2.80 mmol, 45 %), m. p. 144 °C. – ^{1}H NMR (400 MHz, $CDCl_3$) selected data of the tetracoordinate isomer **2a**: δ = 0.33 (s, 6H, Si-CH_3), 3.72 (s, 3H, O-CH_3), selected data of the pentacoordinate isomer **2a′**: δ = 0.27 (s, 6H, Si-CH_3), 3.85 (s, 3H, O-CH_3). – ^{13}C NMR (101 MHz, $CDCl_3$) selected data of the tetracoordinate isomer **2a**: δ = −3.6, −2.5 (Si-CH_3), 55.2 (O-CH_3), selected data of the pentacoordinate isomer **2a′**: δ = 2.8 (Si-CH_3), 55.6 (O-CH_3). – ^{29}Si NMR (79 MHz, $CDCl_3$): δ = −7.3 (**2a**), −52.4 (**2a′**) (79 MHz, CP/MAS): δ = −6.3 (**2a**). – $C_{22}H_{21}NO_3Si$ (375.50): calcd. C 70.37, H 5.64, N 3.73; found C 70.67, H 5.91, N 4.05.

2b: In thf (100 mL) ligand **1** (4.00 g, 12.5 mmol) and triethylamine (3.80 g, 37.6 mmol) were stirred at r. t. and diphenyldichlorosilane (3.25 g, 12.85 mmol) was added

dropwise. The resulting orange mixture was stored at 8 °C overnight. Then the precipitated hydrochloride was filtered off and washed with thf (30 mL). 100 mL of the volatiles were removed from the filtrate under reduced pressure and the remaining solution was allowed to stand overnight to yield orange crystals of **2b** which were filtered off, washed with thf (7 mL) and dried in a vacuum. Yield: 3.55 g (7.11 mmol, 57 %), m. p. 234 °C. – ^{1}H NMR (400 MHz, $CDCl_3$): δ = 3.87 (s, 3H, O-CH_3), 5.77 (d, 1H, ar, $^3J_{HH}$ = 8.0 Hz), 6.35 – 6.45 (m, 2H, ar), 6.74 (d, 1H, $^3J_{HH}$ = 9.2 Hz), 6.81 (d, 1H, ar, $^4J_{HH}$ = 2.4 Hz), 6.95 – 7.50 (mm, 17H, ar). – ^{13}C NMR (101 MHz, $CDCl_3$): δ = 55.7 (O-CH_3), 104.8, 109.2, 116.3, 116.5, 119.6, 120.3, 127.2, 127.3, 128.1, 129.0, 129.5, 129.9, 132.6, 133.5, 134.0, 135.6, 142.4 (ar), 154.1, 161.0, 165.5, 166.1 (ar C-O, C=N). – ^{29}Si NMR (79 MHz, $CDCl_3$): δ = −84.6. – $C_{32}H_{25}NO_3Si$ (499.64): calcd. C 76.93, H 5.04, N 2.80; found C 76.29, H 5.25, N 2.91.

2c: In thf (40 mL) ligand **1** (1.0 g, 3.1 mmol) and triethylamine (0.75 g, 7.4 mmol) were stirred at r. t. and allylphenyldichlorosilane (0.70 g, 3.2 mmol) was added dropwise. The resulting orange mixture was stored at 8 °C for 2 h. Then the precipitated hydrochloride was filtered off and washed with thf (5 mL). The volatiles were removed from the filtrate under reduced pressure and the remaining orange solid was dissolved in diethyl ether (5 mL). This solution was filtered and pentane (3 mL) was added to the clear filtrate. Within 1 week at 8 °C orange crystals of **2c** had formed. The mother liquor was removed with a syringe and the crystals were dried in a vacuum. Yield: 0.58 g (1.3 mmol, 42 %), m. p. 124 °C. – ^{1}H NMR (400 MHz, $CDCl_3$): δ = 1.94 (m, 2H, Si-CH_2), 3.88 (s, 3H, O-CH_3), 4.70 (m, 2H, -CH=CH_2), 5.79 (d, 1H, ar, $^3J_{HH}$ = 8.4 Hz), 5.92 (m, 1H, CH_2-CH=CH_2), 6.30-7.60 (mm, 16H, ar). – ^{13}C NMR (101 MHz, $CDCl_3$): δ = 28.6 (Si-CH_2), 55.7 (O-CH_3), 104.8, 109.0, 112.1, 116.1, 116.7, 119.3, 120.2, 127.2, 127.4, 128.2, 129.0, 129.5, 129.9, 132.5, 133.4 (2×), 135.7, 137.2, 141.2 (ar, CH_2-CH=CH_2), 154.2, 161.2, 165.5, 166.0 (ar C-O, C=N). – ^{29}Si NMR (79 MHz, $CDCl_3$): δ = −76.2. – $C_{29}H_{25}NO_3Si$ (463.61): calcd. C 75.13, H 5.44, N 3.02; found C 74.99, H 5.43, N 2.99.

X-Ray structure analyses

X-Ray structure data were recorded on a Bruker-Nonius-X8-APEX2-CCD diffractometer with MoK_α radiation (λ = 0.71073 nm) and semi-empirical correction (SADABS). The structures were solved with Direct Methods (SHELXS-97) and refined by full-matrix least-squares methods (refinement for all reflections against F^2 with SHELXL-97). All non-hydrogen atoms were refined anisotropically. Hydrogen atoms were placed in idealized positions and refined isotropically (riding model). Hydrogen atoms of OH and NH groups were found by residual electron density and refined isotropically.

In the structure of **2a** the space groups $P2_1/m$ (Z = 2, virtual bisecting plane in the two-molecules) and $P2_1$ (Z = 2, twofold screw axis, the same kind of disorder) were simulated. $P2_1/m$ together with Z = 2 is impossible due to the absence of a bisecting plane within molecule **2a**. In order to account for Z = 2 and the missing anomalous diffraction, the structure was solved and refined in the triclinic space group $P\bar{1}$. The diffraction pattern exhibited weak reflections with non-integer h-indices. Therefore, structure solution and refinement was also tried using a cell with doubled a axis. Attempts to refine the structure in other space groups than $P\bar{1}$ (*e. g.* using the initial unit cell in space group $P2_1$ or using a doubled unit cell and space groups Pc or $P2_1/c$) led to the same result of molecular disorder which could not be resolved by inclusion of racemic twinning in case of the non-centrosymmetric space groups. The diffraction pattern exhibited only very broad reflections which underline the presence of disturbances such as heavy disorder in the crystal, which make determination of the correct space group impossible. The disorder in the structure of **2a** was resolved using numerous restraints [16]: SAME was applied for fragments [O1, C1-C6], [O3, C15-C20], [N1, C7-C13] to fit the corresponding fragments of the disordered counterpart; bond lengths Si1-C21, Si1-C22 were restrained to the same lengths as in the corresponding counterpart and the aromatic bond lengths in [C8-C13] were restrained to be identical using SADI. Identical anisotropic displacement parameters for atoms in similar positions were applied.

Selected data of structure determination and refinement are presented in Table 1. Crystallographic data (excluding structure factors) for the structures reported in this paper have been deposited with the Cambridge Crystallographic Data Centre as supplementary publication no. CCDC-611921 (**1**), CCDC-611918 (**2a**), CCDC-611919 (**2b**), and CCDC-611920 (**2c**). Copies of the data can be obtained free of charge from The Cambridge Crystallographic Data Centre *via* www.ccdc.cam.ac.uk/data_request/cif.

Acknowledgements

This work was financially supported by the German Science Foundation (DFG) and the German Chemical Industry Fund.

[1] C. Chuit, R. J. P. Corriu, C. Reye, J. C. Young, *Chem. Rev.* **1993**, *93*, 1371.

[2] A. Kolomeitsev, G. Bissky, E. Lork, V. Movchun, E. Rusanov, P. Kirsch, G.-V. Röschenthaler, *Chem. Commun.* **1999**, 1107.

[3] a) E. P. A. Couzijn, M. Schakel, F. J. J. de Kanter, A. W.

Ehlers, M. Lutz, A. L. Spek, K. Lammertsma, *Angew. Chem.* **2004**, *116*, 3522; *Angew. Chem., Int. Ed.* **2004**, *43*, 3440; b) S. Deerenberg, M. Schakel, A. H. J. F. de Keijzer, M. Kranenburg, M. Lutz, A. L. Spek, K. Lammertsma, *Chem. Commun.* **2002**, 348.

[4] a) M. E. Mowery, P. DeShong, *J. Org. Chem.* **1999**, *64*, 3266; b) C. Wolf, R. Lerebours, *Org. Lett.* **2004**, *6*, 1147; c) S. Riggleman, P. DeShong, *J. Org. Chem.* **2003**, *68*, 8106; d) W. M. Seganish, P. DeShong, *J. Org. Chem.* **2004**, *69*, 1137; e) S. E. Denmark, R. F. Sweis, *Acc. Chem. Res.* **2002**, *35*, 835.

[5] a) N. Kano, M. Yamamura, T. Kawashima, *J. Am. Chem. Soc.* **2004**, *126*, 6250; b) N. Aoyama, T. Hamada, K. Manabe, S. Kobayashi, *J. Org. Chem.* **2003**, *68*, 7329; c) A. V. Malkov, M. Orsini, D. Pernazza, K. W. Muir, V. Langer, P. Meghani, P. Kocovský, *Org. Lett.* **2002**, *4*, 1047; d) M. Kira, T. Taki, H. Sakurai, *J. Org. Chem.* **1989**, *54*, 5674; e) M. Kira, K. Sato, H. Sakurai, *J. Am. Chem. Soc.* **1990**, *112*, 257; f) M. Kira, L. C. Zhang, C. Kabuto, H. Sakurai, *Organometallics* **1998**, *17*, 887.

[6] J. Wagler, T. Doert, G. Roewer, *Angew. Chem.* **2004**, *116*, 2495; *Angew. Chem. Int. Ed.* **2004**, *43*, 2441.

[7] a) I. Kalikhman, B. Govstevskii, M. Botoshansky, M. Kaftory, C. A. Tessier, M. J. Panzner, W. J. Youngs, D. Kost, *Organometallics* **2006**, *25*, 1252; b) D. Kost, V. Kingston, B. Gostevskii, A. Ellern, D. Stalke, B. Walfort, I. Kalikhman, *Organometallics* **2002**, *21*, 2293; c) D. Kost, V. Kingston, B. Gostevskii, V. Pestunovich, D. Stalke, B. Walfort, I. Kalikhman, *Organometallics* **2002**, *21*, 4468.

[8] a) J. Wagler, G. Roewer, *Z. Naturforsch.* **2005**, *60b*, 709; b) J. Wagler, U. Böhme, E. Brendler, S. Blaurock, G. Roewer, *Z. Anorg. Allg. Chem.* **2005**, *631*, 2907.

[9] J. Wagler, G. Roewer, *Z. Naturforsch.* **2006**, *61b*, 1406.

[10] J. Wagler, U. Böhme, E. Brendler, G. Roewer, *Organometallics* **2005**, *24*, 1348.

[11] J. Wagler, *Organometallics* **2007**, *26*, in press.

[12] J. Wagler, U. Böhme, E. Brendler, G. Roewer, *Z. Naturforsch.* **2004**, *59b*, 1348.

[13] O. Seiler, C. Burschka, S. Metz, M. Penka, R. Tacke, *Chem. Eur. J.* **2005**, *11*, 7379.

[14] a) T. K. Prakasha, A. Chandrasekaran, R. O. Day, R. R. Holmes, *Inorg. Chem.* **1996**, *35*, 4342; b) E. Gómez, V. Santes, V. de la Luz, N. Farfán, *J. Organomet. Chem.* **1999**, *590*, 237; c) E. Gómez, V. Santes, V. de la Luz, N. Farfán, *J. Organomet. Chem.* **2001**, *622*, 54.

[15] R. Atkins, G. Brewer, E. Kokot, G. M. Mockler, E. Sinn, *Inorg. Chem.* **1985**, *24*, 127.

[16] For explanation of SAME and SADI restraints see the SHELX-97 manual.